In-Situ Time-of-Flight Neutron Diffraction Study of High-Temperature α-to-β Phase Transition in Elemental Scandium

DANIEL R. KAMMLER, MARK A. RODRIGUEZ, RALPH G. TISSOT, DONALD W. BROWN, BJØRN CLAUSEN, and THOMAS A. SISNEROS

Lattice parameters for both hcp α-Sc and bcc β-Sc were determined between 1200 °C and 1400 °C from time-of-flight (TOF) neutron diffraction data collected from an elemental Sc sample vacuum sealed inside a niobium crucible. On heating, the high-temperature β-Sc phase first appeared between 1340 °C and 1350 °C, close to the reported transition temperature of 1337 °C. The lattice constants of hcp α-Sc were found to vary between $a = 3.3522(4)$ Å, $c = 5.3807(7)$ Å at 1200 °C and $a = 3.3579(6)$ Å, $c = 5.398(1)$ Å at 1340 °C. The lattice constants of bcc β-Sc were found to vary between $a = 3.752(2)$ Å at 1350 °C and $a = 3.7572(8)$ Å at 1400 °C. The average thermal expansion coefficient for the bcc β-Sc phase was 1.61×10^{-5} °C^{-1} over the temperature range 1360 °C to 1400 °C. The average thermal expansion coefficient along the a-axis of hcp α-Sc between 1200 °C and 1340 °C was 1.46×10^{-5} °C^{-1}. The average thermal expansion coefficient along the c-axis of hcp α-Sc between 1200 °C and 1340 °C was 2.22×10^{-5} °C^{-1}.

DOI: 10.1007/s11661-008-9642-y

I. INTRODUCTION

SCANDIUM is often used as an additive in aluminum alloys. The addition of Sc dramatically increases the recrystallization temperature of the alloy through formation of an Al_3Sc intermetallic phase.[1] Thus, aluminum alloys that display fine-grain microstructure along with Al_3Sc precipitates can be produced with superior strengths.[1,2] Recently, Sc has been suggested as a key component in multilayer Cr/Sc mirrors for use in X-ray microscopy.[3,4] Elemental scandium has the hcp crystal structure at room temperature. Spedding *et al*. reported lattice constants of $a = 3.308(1)$ Å and $c = 5.267(3)$ Å at 298 K for Sc.[5] At high pressures, other polymorphs of scandium have been reported.[6,7] Scandium is documented to have a high-temperature phase transition at 1337 °C.[8] Beaudry and Daane concluded that the low-temperature hcp Sc phase transformed to a high-temperature bcc phase. Their conclusions were based on metallographic analysis of Sc-Ti alloy samples quenched from the beta phase region of the Sc-Ti system.[9] However, they were unable to show direct structural evidence of the bcc phase (*via in-situ* X-ray diffraction (XRD)) due to the high vapor pressure of scandium at the temperatures of interest. It is generally accepted that the high-temperature β-Sc phase has the bcc structure and transforms to the hcp α-Sc phase *via* the mechanism described by Burgers[10] for the bcc to hcp transition in Zr.[11] Surprisingly, there does not appear to be any reported study documenting the α to β phase transition in Sc by direct *in-situ* X-ray or neutron diffraction. Indeed, the only experimentally determined high-temperature structural information we have found for the β-Sc phase is a lattice constant of 3.765(5) Å at 1673 K reported by Petry *et al*. during a phonon dispersion study of β-Sc.[12] In this article, we present the results of a high-temperature *in-situ* neutron diffraction study of the phases, lattice constants, and thermal expansion coefficients of the α and β Sc phases between 1200 °C and 1400 °C.

II. EXPERIMENTAL

Scandium metal pieces of 99.7 wt pct purity (Alfa Aesar in Ward Hill, MA) ranging in size from 0.5 to 18.5 mm were used in this study. These Sc pieces were pulverized in a Spex (Metuchen, NJ) model 6700 cryogenic mill employing a 304L stainless steel vial. The end caps and impact rod of the mill were fabricated from a 440C martensitic steel. The Sc pieces were placed inside the vial with the impact rod and agitated under liquid nitrogen (77 K) for 90 minutes. This yielded Sc particulates with platelike morphology. These particulates were sieved to a final particulate size range of 100 μm to 1 mm.

XRD of the sieved Sc powder was performed using a Siemens (Madison, WI) D500 diffractometer equipped with a sealed-tube Cu X-ray source, a diffracted-beam

DANIEL R. KAMMLER, MARK A. RODRIGUEZ, and RALPH G. TISSOT, Members of Technical Staff, are with Sandia National Laboratories, Albuquerque, NM 87185. DONALD W. BROWN, BJØRN CLAUSEN, and THOMAS A. SISNEROS, Technical Staff Members, are with Los Alamos National Laboratory, Los Alamos, NM 87545. Contact e-mail: drkamml@sandia.gov
Manuscript submitted April 16, 2008.

graphite monochromator, and a scintillation detector. The initial batch of Sc powder was scanned at room temperature between 15 and 125 deg in 2θ with a step size of 0.04 deg and a counting time of 18 seconds per step. The resulting pattern indicated phase pure Sc within the sensitivity limit of the instrument. This pattern was later used for Rietveld structural analysis. Subsequent batches of Sc powder produced with the preceding milling process were scanned between 10 and 60 deg 2θ with a step size of 0.04 deg and a counting time of 1 second per step. As before, only hcp Sc was observed in these XRD patterns.

In order to avoid evaporation at the temperature range of interest, the Sc powder had to be sealed into crucibles made from a nonreacting refractory material with minimal neutron absorption problems. Niobium met all of these requirements. While a eutectic has been reported to form in the Nb-Sc system at 1500 °C (97 pct Sc and 3 pct Nb), no intermetallic compounds between Nb and Sc are known to form, the solubility of Nb in β-Sc is between 0.3 and 0.4 pct, and the solubility of Nb in α-Sc is significantly less than 0.3 pct.[13,14] The solubility of Sc in Nb is reported to be less than 0.1 pct.[13,14]

The sieved Sc particulates were loaded into a specially machined Nb cylinder made by Metal Technology Incorporated (Albany, OR). The Nb cylinder was open on one end, which had an outer diameter of 11.8 mm, an inner diameter of 10.0 mm, and a height of 25.4 mm. The Nb lid fit tightly onto the top of the cylinder. A total of 0.648 g of Sc particulates was loaded into this Nb canister; it was approximately half-full after loading. The Nb canister was then pumped down below 10^{-4} mbar before electron beam welding the Nb lid onto the canister to seal the Sc particulates in vacuum, ready for neutron diffraction analysis.

Time-of-flight (TOF) neutron diffraction was performed on the spectrometer for materials research at temperature and stress (SMARTS) beamline at the LANSCE facility at Los Alamos National Laboratory. Details of the SMARTS instrument have been fully reported elsewhere.[15] We provide a brief description of the experimental setup used for this *in-situ* analysis. Diffraction patterns having a range of 0.5 to 4 Å were measured using two detector banks located 90 deg from the incident neutron beam. The Nb cylinder with the Sc powder rested on top of a boron nitride plate 8-mm wide and 5-mm thick. There was a hole in the plate through which a thermocouple penetrated and contacted the niobium can. Initially, the sample was heated from room temperature (~25 °C) to 1150 °C at a rate of 50 °C/min. Afterward, the sample was heated to 1200 °C and subsequent temperatures at a rate of 10 °C/min. Data sets were collected at each hold temperature in approximately 5-minute increments, starting at 1200 °C. It took approximately 5 minutes to collect data sets with adequate counting statistics. Ten data sets were collected at each temperature to observe any time-dependent changes in the diffraction pattern. Because no time dependence was observed, the 10 data sets at each temperature were then merged into a single data set, thereby maximizing the signal-to-noise ratio of the data for each temperature step.

Both the initial XRD and the raw TOF neutron diffraction data were refined using the generalized structure analysis system (GSAS)[16] and the GUI interface of Toby.[17] For the XRD data, two cell constants (a-axis and c-axis), an isotropic displacement parameter (U_{iso}), a strain-broadening parameter, four March–Dollase orientation parameters, and six additional fitting parameters were refined. For the neutron diffraction data, the refined phases included bcc Nb, hcp Sc (up through 1370 °C), and bcc Sc (at 1350 °C and above). The refined parameters included the cell constants, weight fractions, and isotropic displacement parameters (U_{iso}) of each phase. The texture of the hcp α-Sc and the bcc Nb was modeled using spherical harmonics. An additional profile fitting parameter related to peak width was also refined.

III. RESULTS AND DISCUSSION

A. *XRD and TOF Neutron Diffraction of Sc Powders at Ambient Temperature*

Figure 1 shows the refined XRD pattern collected at room temperature of the sieved Sc powder after milling. An R_p of 12.73 pct was obtained for the fit. Only hexagonal Sc was observed. It is also obvious from Figure 1 that there is a strong (002) preferred orientation. The (002) diffraction vector is perpendicular to the plane of the platelike Sc particulates. When these particulates were loaded into the Nb cylinder, they tended to orient themselves such that the normal to the Sc plate is parallel with the axis of the Nb cylindrical crucible. The XRD refinement also showed an enhanced (103) peak. Both the (002) and (103) preferred orientation directions were modeled within the GSAS refinement, with the (002) direction dominating the preferred orientation dependence of the powder.

Figure 2 shows the results of a GSAS Rietveld refinement of TOF neutron diffraction data collected from the Sc sample. This histogram was collected at room temperature, prior to heating. This plot shows peaks for the hcp α-Sc phase along with Nb peaks from

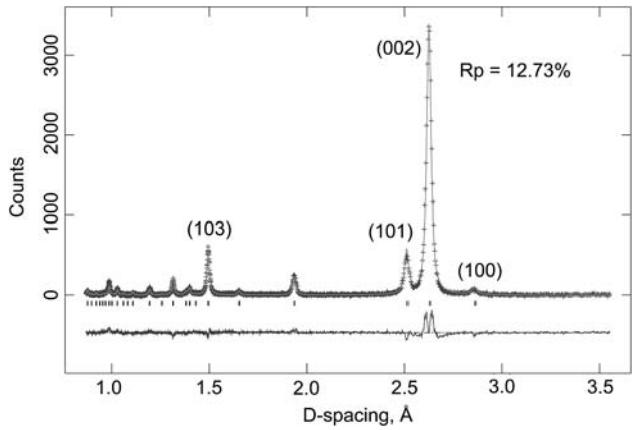

Fig. 1—Rietveld refinement of XRD data collected from Sc powder after 90 min of cryogenic milling (data collected at room temperature).

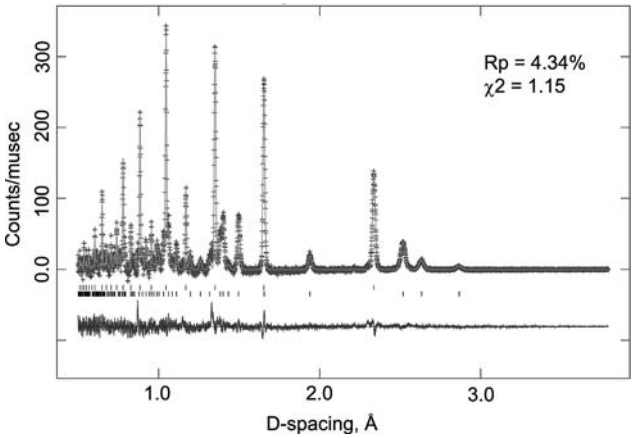

Fig. 2—Rietveld refinement of TOF Sc neutron powder diffraction data taken at room temperature prior to heating. Top markers correspond to Nb and bottom markers correspond to α-Sc.

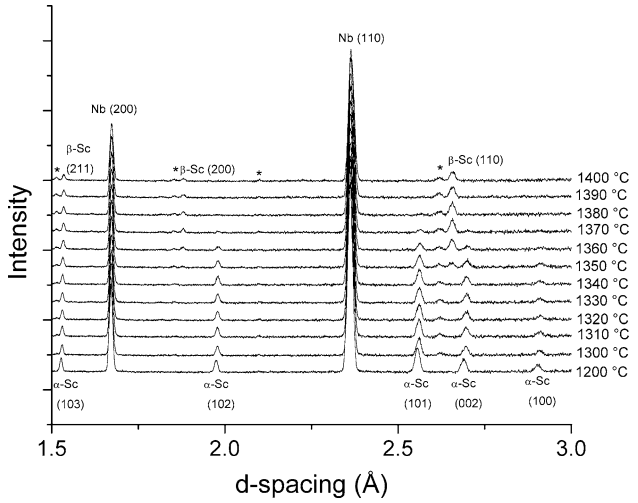

Fig. 3—Stack plot of TOF neutron diffraction histograms collected from 1200 °C to 1400 °C (refer to the text for details).

the sample container. The hcp α-Sc was found to have $a = 3.3098(5)$ Å and $c = 5.266(1)$ Å. This compares well with the lattice constants of $a = 3.308(1)$ Å and $c = 5.267(3)$ Å reported by Spedding *et al.*[5]

B. *Heating of Sc Powders between 1200 °C and 1400 °C*

Figure 3 shows a stack plot of TOF histograms collected between 1200 °C and 1400 °C. Only hcp α-Sc is present at 1340 °C and below. The transition to the β-Sc phase begins between 1340 °C and 1350 °C and is complete between 1370 °C and 1380 °C. Table I shows a summary of the GSAS refinement statistics, cell constants, phase fractions, and U_{iso} for the histograms shown in Figure 3. Figure 4 shows the Rietveld refinement of TOF Sc data collected at 1380 °C during heating. There is no evidence of the α-Sc at 1380 °C.

A few weak peaks (marked with asterisks) appear at 2.62, 2.1, 1.85, and 1.51 Å in Figure 3. The peak at 2.1 Å is probably from the boron nitride plate on which the Nb crucible rested. The remaining peaks marked with asterisks can all be indexed to a bcc unit cell with a slightly smaller cell constant of 3.70 Å. We have observed that when the Sc powder is heated to 1400 °C, the particulates sinter together and form a compact that pulls away from the crucible walls as its density increases. The Nb and Sc have covalent metallic radii of 1.342 and 1.439 Å, respectively.[18] Terkhova reported that Nb stabilizes β-Sc down to 1325 °C, β-Sc dissolves between 0.3 and 0.4 at. pct of Nb, and α-Sc dissolves significantly less than 0.3 pct Nb.[14] Consequently, the additional peaks that can be assigned to the bcc unit cell with $a = 3.70$ Å may come from a small amount of a bcc Sc-Nb solid solution on the walls of the crucible (the majority of the Sc is not in contact with the walls once it has pulled away). The fact that these peaks can be assigned to a slightly smaller bcc unit cell than the bcc β-Sc is consistent with the smaller atomic radius of Nb relative to the Sc noted previously. The appearance of the peaks from the small amount of Sc-Nb solid solution on the crucible walls at temperatures below the 1350 °C to 1370 °C region, where both α and β Sc phases are observed, is consistent with the earlier report that Nb stabilizes the bcc Sc phase to lower temperatures.

While the α to β phase transition in elemental Sc has been reported to occur at 1337 °C,[8] both phases are present in the 1350 °C, 1360 °C, and 1370 °C data sets. Assuming that the Nb has only minimal contact with the Sc powder compact than the Sc makes up a one-component system. Gibb's phase rule only allows the existence of α-Sc and β-Sc at a single temperature (assuming pressure is fixed) in this system at equilibrium. There are at least a couple possible explanations for the observation of α-Sc and β-Sc at 1350 °C, 1360 °C, and 1370 °C. A temperature gradient could explain the presence of both phases at once. In order to test this hypothesis, the slit size was cut in half at 1370 °C in order to sample a smaller fraction (in height) of the Nb crucible with the neutron beam. Both α-Sc and β-Sc phases were still visible. While this result makes a large temperature gradient somewhat less likely, the fact that the Nb crucible was in contact with the boron nitride plate at the bottom and only vacuum at the top might allow for a temperature gradient that was sufficient to stabilize both phases within the smaller volume sampled by the reduced beam size. The presence of pockets and voids within the coarsely packed powder might also contribute to the presence of a temperature gradient.

Another possible explanation for the presence of both phases is the presence of a minor impurity in the Sc. An additional impurity would bring the total number of components to two (scandium plus an impurity) and thereby increase the maximum number of phases that could be present over a temperature range to two in accordance with Gibb's phase rule. One possible impurity is oxygen. The vendor (Alfa Aesar) supplied analysis with the Sc indicated that there was 423 ppm of oxygen present in the lot of Sc used in this experiment. Additional oxygen could have been absorbed into the Sc powder during or after the pulverization process after

Table I. Refined Parameters and Fitting Statistics from GSAS Refinement of Data in Figures 2 and 3

Temperature (°C)	α-Sc Cell Constants a (Å) c (Å)	β-Sc Cell Constants a (Å)	Fraction of β-Sc	U_{iso} α-Sc	U_{iso} β-Sc	χ^2	R_{wp} (Pct)
25	3.3098(5) 5.266(1)	—	0	0.0147(6)	—	1.15	5.96
1200	3.3522(4) 5.3807(7)	—	0	0.026(2)	—	1.436	2.7
1300	3.3566(5) 5.392(1)	—	0	0.027(3)	—	1.476	2.82
1310	3.3567(5) 5.394(1)	—	0	0.027(3)	—	1.533	2.78
1320	3.3571(6) 5.396(1)	—	0	0.028(3)	—	1.557	2.86
1330	3.3577(6) 5.396(1)	—	0	0.028(3)	—	1.523	2.84
1340	3.3579(6) 5.398(1)	—	0	0.026(3)	—	1.522	2.8
1350	3.3577(8) 5.401(2)	3.752(2)	0.1	0.028(4)	0.03(2)	1.526	2.81
1360	3.355(1) 5.408(2)	3.755(1)	0.3	0.029(7)	0.031(8)	1.506	2.8
1370	3.357(3) 5.41(1)	3.7559(6)	0.7	0.022(5)	0.025(3)	1.566	2.85
1380	—	3.7560(7)	1	—	0.025(3)	1.595	2.89
1390	—	3.7571(7)	1	—	0.018(5)	1.532	2.82
1400	—	3.7572(8)	1	—	0.019(6)	1.397	2.77

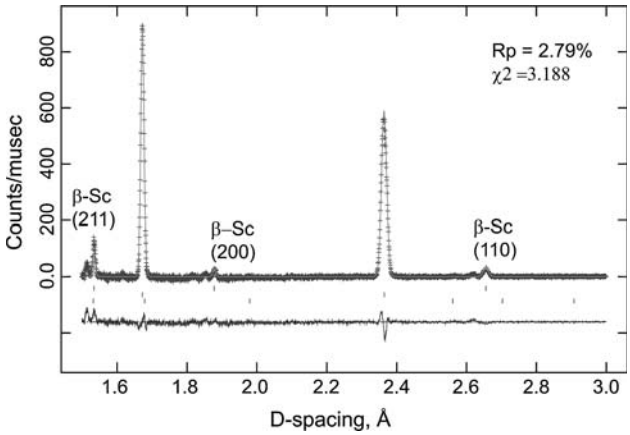

Fig. 4—GSAS Rietveld refinement of Sc during heating at 1380 °C. Top markers correspond to β-Sc, middle markers correspond to Nb, and bottom markers to α-Sc.

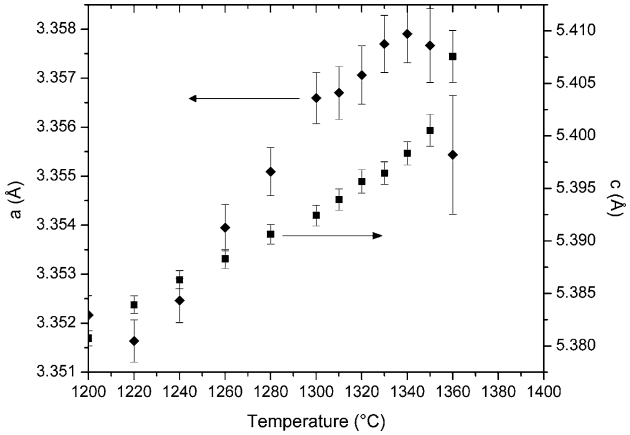

Fig. 5—Cell constants (a and c) for hcp α-Sc *vs* temperature.

which it had a significantly larger surface area than the starting chunks of material. Although a pressure of 10^{-4} mbar was reached prior to sealing the Sc in the Nb crucible, oxygen stored in a layer of Sc_2O_3 on the Sc surface would not be pumped out. In order to put an upper bound on the oxygen concentration, one could assume that the entire 0.648 g of sieved Sc material was made of the smallest 100-μm particles and that these particles were each coated with Sc_2O_3 0.2-μm thick (0.2 μm or thicker films of Sc_2O_3 would likely have been detected in the initial XRD pattern). The total concentration of oxygen after equilibrium was reached would be approximately 0.5 wt pct or 5000 wt ppm. It is apparent from the Ti-O phase diagram that as little as 0.5 wt pct of oxygen can stabilize Ti in the alpha phase by 20 °C.[13,19] Given that titanium has a similar metallurgy to scandium, the observation of both α-Sc and β-Sc at 1350 °C, 1360 °C, and 1370 °C may be explained by the existence of a similar level of oxygen in the Sc used in this study.

C. *Change in Lattice Constants during Heating and Cooling*

Figures 5 and 6 show the cell constants for the hcp α-Sc and bcc β-Sc *vs* temperature. Figure 5 shows how the c-axis expands and the a-axis contracts as the hcp α-Sc transforms into bcc β-Sc. The presence of an impurity such as oxygen may result in a slight increase of the lattice constants relative to what would be

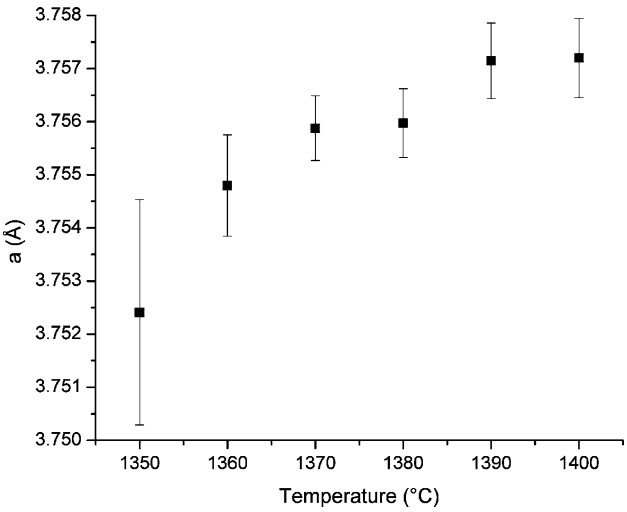

Fig. 6—Cell constant for bcc β-Sc *vs* temperature.

observed in pure Sc. The *a* and *c* cell constants in hcp Ti increase 0.01 and 0.005 Å, respectively, relative to their values in pure Ti when 1 wt pct of oxygen is dissolved in the metal.[20] Given the possible levels of oxygen contamination in the Sc used in this study, and the similar metallurgy of Ti and Sc, one might expect the lattice parameters reported in this study to be larger than those for pure Sc metal by a similar level.

The mean coefficients of thermal expansion (CTEs) along *a* and *c* in hcp Sc between 1200 °C and 1340 °C were found to be 1.46×10^{-5} °C^{-1} and 2.22×10^{-5} °C^{-1}, respectively. Geiselman reported a CTE of 1.786×10^{-5} 1/°C between 600 °C and 950 °C from dilatometer data collected on a Sc rod heated in an Ar atmosphere.[21] Mardon *et al.* reported CTEs along *a* and *c* of 1.66×10^{-5} 1/°C and 1.73×10^{-5} 1/°C, respectively, at 800 °C from X-ray powder diffraction data collected from Sc fillings heated in a sealed thin-walled silica tube under vacuum.[22] The average CTE for bcc Sc between 1360 °C and 1400 °C was found to be 1.61×10^{-5} °C^{-1}.

IV. CONCLUSIONS

TOF neutron diffraction data were collected between 1200 °C and 1400 °C from elemental Sc powder prepared *via* cryomilling. Both hcp α-Sc and bcc β-Sc phases were observed at 1350 °C, 1360 °C, and 1370 °C. Only bcc β-Sc was observed at 1380 °C and above. The existence of both phases over the observed temperature range could be due to the presence of a temperature gradient or a minor impurity such as oxygen. The average thermal expansion coefficient for the bcc β-Sc phase was determined to be 1.61×10^{-5} 1/°C over the temperature range 1360 °C to 1400 °C. The average thermal expansion coefficients along the *a*-axis and *c*-axis of hcp α-Sc between 1200 °C and 1340 °C were determined to be 1.46×10^{-5} 1/°C and 2.22×10^{-5} 1/°C, respectively.

ACKNOWLEDGMENTS

Sandia is a multiprogram laboratory operated by Sandia Corporation, a Lockheed Martin Company, for the United States Department of Energy (DOE), under Contract No. DE-AC04-94AL85000. This work has benefited from the use of the Lujan Neutron Scattering Center at LANSCE, which is funded by the Office of Basic Energy Sciences (DOE). Los Alamos National Laboratory is operated by Los Alamos National Security LLC under DOE Contract No. DE-AC52-06NA25396.

REFERENCES

1. V.G. Davydov, T.D. Rostova, V.V. Zakharov, Y.A. Filatov, and V.I. Yelagin: *Mater. Sci. Eng. A*, 2000, vol. 280, pp. 30–36.
2. V.I. Elagin, V.V. Zakharov, and T.D. Rostova: *Met. Sci. Heat Treat.*, 1992, vol. 34, pp. 37–45.
3. T. Gorelik, U. Kaiser, T. Kuhlmann, S. Yulin, and W. Richter: *Appl. Surf. Sci.*, 2004, vol. 230, pp. 1–7.
4. T. Kuhlmann, S. Yulin, T. Feigl, N. Kaiser, T. Gorelik, U. Kaiser, and W. Richter: *Appl. Opt.*, 2002, vol. 41, pp. 2048–52.
5. F.H. Spedding, A.H. Daane, G. Wakefield, and D.H. Dennison: *Trans. TMS-AIME*, 1960, vol. 218, pp. 608–11.
6. Y.C. Zhao, F. Porsch, and W.B. Holzapfel: *Phys. Rev. B*, 1996, vol. 54, pp. 9715–20.
7. W.A. Grosshans, Y.K. Vohra, and W.B. Holzapfel: *J. Magn. Magn. Mater.*, 1982, vol. 29, pp. 282–86.
8. *Scandium: Its Occurrence, Chemistry, Physics, Metallurgy, Biology, and Technology*, C.T. Horovitz, K.A. Gschneidner, G.A. Melson, D.H. Youngblood, and H.H. Schock, eds., Academic Press, London, 1975, p. 81.
9. B.J. Beaudry and A.H. Daane: *Trans. TMS-AIME*, 1962, vol. 224, pp. 770–75.
10. W.G. Burgers: *Physica*, 1934, vol. 1, pp. 561–86.
11. M. Sanati, A. Saxena, and T. Lookman: *Phys. Rev. B*, 2001, vol. 64, pp. 092101–092104.
12. W. Petry, J. Trampenau, and C. Herzig: *Phys. Rev. B*, 1993, vol. 48, pp. 881–86.
13. *Binary Alloy Phase Diagrams*, 2nd ed., ASM INTERNATIONAL, Materials Park, OH, 1996.
14. V.F. Terkhova: *Fiz. Khim. Redkikh Metallov.*, 1972, pp. 66–76.
15. M.A.M. Bourke, D.C. Dunand, and E. Ustundag: *Appl. Phys. A*, 2002, vol. 74, pp. S1707–S1709.
16. A.C. Larson and R.B.V. Dreele: Los Alamos National Laboratory Report No. LAUR 86–748, Los Alamos National Laboratory, Los Alamos, NM, 2004.
17. B.H. Toby: *J. Appl. Cryst.*, 2001, vol. 34, pp. 210–13.
18. L.S. Darken and R.W. Gurry: *Physical Chemistry of Metals*, McGraw-Hill Book Company, New York, NY, 1953, p. 61.
19. T. Tsuji: *J. Nucl. Mater.*, 1997, vol. 247, pp. 63–71.
20. S. Andersson, B. Collen, U. Kuylenstierna, and A. Magneli: *Acta Chemica Scandinavica*, 1957, vol. 11, pp. 1641–52.
21. D. Geiselman: *J. Less-Common Met.*, 1962, vol. 4, pp. 362–75.
22. P.G. Mardon, J.L. Nichols, J.H. Pearce, and D.M. Poole: *Nature*, 1961, vol. 189, pp. 566–68.